Atmos. Meas. Tech. Discuss., 4, 691–713, 2011
www.atmos-meas-tech-discuss.net/4/691/2011/
doi:10.5194/amtd-4-691-2011

Atmospheric Measurement Techniques Discussions

Droplet activation, separation, and compositional analysis: laboratory studies and atmospheric measurements

N. Hiranuma[1], M. Kohn[2], M. S. Pekour[1], D. A. Nelson[1], J. E. Shilling[1], and D. J. Cziczo[1,*]

[1]Atmospheric Sciences and Global Change Division, Pacific Northwest National Laboratory, 902 Battelle Blvd., Richland, Washington, USA
[2]Institute for Atmospheric and Environmental Sciences, Goethe-University Frankfurt am Main, Frankfurt, Germany
[*]now at: Earth, Atmospheric and Planetary Sciences, Massachusetts Institute of Technology, 77 Massachusetts Ave., Cambridge, Massachusetts, USA

Received: 1 December 2010 – Accepted: 13 January 2011 – Published: 24 January 2011

Correspondence to: D. J. Cziczo (djcziczo@mit.edu)

Published by Copernicus Publications on behalf of the European Geosciences Union.

Abstract

Droplets produced in a cloud condensation nucleus chamber as a function of supersaturation have been separated from unactivated aerosol particles using counterflow virtual impaction. Residual material after droplets were evaporated was chemically analyzed with an Aerodyne Aerosol Mass Spectrometer and the Particle Analysis by Laser Mass Spectrometry instrument. Experiments were initially conducted to verify activation conditions for monodisperse ammonium sulfate particles and to determine the resulting droplet size distribution as a function of supersaturation. Based on the observed droplet size, the counterflow virtual impactor cut-size was set to differentiate droplets from unactivated interstitial particles. Validation experiments were then performed to verify that only droplets with sufficient size passed through the counterflow virtual impactor for subsequent analysis. A two-component external mixture of monodisperse particles was also exposed to a supersaturation which would activate one of the types (ammonium sulfate) but not the other (polystyrene latex spheres). The mass spectrum observed after separation indicated only the former, validating separation of droplets from unactivated particles. Results from atmospheric measurements using this technique indicate that aerosol particles often activate predominantly as a function of particle size. Chemical composition is not irrelevant, however, and we observed enhancement of sulfate in droplet residuals using single particle analysis.

1 Introduction

Among the most uncertain processes in our current understanding of the climate system is the interaction of aerosol particles with water vapor to form clouds (IPCC, 2007). Changes in particle properties can affect clouds in several ways. For example, an increase in the number of particles in the presence of a constant amount of water vapor can result in more but consequently smaller droplets. Smaller and more numerous droplets resulting in more reflective clouds is known as the 1st indirect or Twomey

AMTD
4, 691–713, 2011

effect (Twomey, 1974). Smaller droplets also initiate precipitation less effectively and this is called the 2nd indirect or Albrect effect (Squires, 1958; Albrect, 1989). More recently, Stevens and Feingold (2009) suggested that aerosol/cloud interactions are more complicated with both micro- and macrophysical buffers existing in the system. In all cases a more complete understanding of how particles form droplets is required to make headway in our understanding of climate.

The formation of droplets by particles when the vapor pressure of water is raised above saturation is theoretically well described. The vapor pressure over a small droplet is always larger than that over a planar water surface due to its curvature; this is known as the Kelvin effect (Seinfeld and Pandis, 2006). Nascent droplets are not pure water, however, and normally contain soluble material from the aerosol from which they originated. These solutes reduce the vapor pressure over the droplet according to Raoult's law. The combination of these two effects leads to Köhler theory which predicts the critical supersaturation which must be overcome in order for a particle to activate as a droplet. This critical supersaturation is therefore a function both of the particle size and composition (Seinfeld and Pandis, 2006).

While Köhler theory is successful in predicting the supersaturation required to activate pure particles of e.g., inorganic salts, atmospheric particles are most often complex mixtures of soluble and insoluble components (Murphy et al., 1998). For this reason, techniques to measure the abundance of cloud condensation nuclei (CCN) have been developed. These so-called CCN chambers (CCNCs) pass aerosol particles through a region where they are exposed to a controllable supersaturation (Roberts and Nenes, 2005). Such chambers therefore do not explicitly rely on theory but instead measure the abundance of CCN, often as a function of supersaturation, within an airmass. In the case of laboratory studies, a CCNC can be utilized with other instruments to determine activation conditions for a given particle type as a function of e.g., size (e.g., Moore et al., 2010).

One use of CCN abundance data is the formation of simple parameterizations of cloud drop number, which can be used at minimal computational expense in models

AMTD
4, 691–713, 2011

(Lohmann and Feichter, 2005). Dusek et al. (2006) produced a simple parameterization by noting that in some cases size was a more important determinate of CCN formation than chemistry. Dusek et al. (2006) considered airmasses with predominantly aged continental aerosol particles and, despite the compositional similarity, at times size only captured ~84% of the CCN variability. More recent research, especially that on more diverse particulate sources, has indicated chemistry does plays a large role in CCN variability. Nenes et al. (2002) showed in a model study that chemical effects can rival the 1st indirect effect in terms of radiative forcing. Petters and Kreidenweis (2007) suggested a single parameter, κ, to represent compositional effects on both hygroscopic growth below saturation and CCN activity. Values of κ indicate a large difference between hygroscopic inorganic species (e.g., NaCl) which largely follows Köhler theory (0.5–1.4) and less active organics (0.01–0.5). Petters and Kreidenweis (2007) determined κ values for atmospheric particles in a range between 0.1 and 0.9. Rose et al. (2010) found somewhat lower values in the highly polluted conditions of Guangzhou, China, 0.1–0.5. The field study κ average was observed to drop from 0.3 to 0.2 in the presence of significant organic-rich biomass burning.

These and other field studies have been dependant on parallel measurements of chemical composition (i.e., the number of CCN and particulate chemical composition were determined separately). Alternately, studies where the effect of composition on CCN formation was directly measured relied on particle generation from a known material in a laboratory setting. The problem with this strategy is that laboratory-generated particles do not undergo the complex processes associated with atmospheric aging that may change composition and surface properties (e.g., Gard et al., 1998; Laskin et al., 2005). Moreover, only a limited amount of particle types can be investigated in a laboratory.

We have coupled a CCNC to a counterflow virtual impactor (CVI) in order to form droplets as a function of supersaturation and separate them for subsequent direct analysis. We then evaporate the condensed-phase water in order to determine the size and composition of the aerosol particles which formed the droplets using an Aerodyne

AMTD
4, 691–713, 2011

Aerosol Mass Spectrometer (AMS) and the Particle Analysis by Laser Mass Spectrometry (PALMS) instrument. Laboratory studies were conducted on particle types with known critical supersaturations in order to validate this technique. Direct measurements of the effect of composition on CCN formation were then conducted with atmospheric aerosol particles.

2 Methodology

A schematic of the experimental setup is shown in Fig. 1. A CCNC, commercially available from Droplet Measurement Technologies (Model 200-013, Boulder, CO), was used to activate droplets from incoming aerosol particles as a function of supersaturation from 0.07–0.5%. A full description of the instrument is available in Roberts and Nenes (2005) with calibration procedures given by Lance et al. (2006), Rose et al. (2008) and Shilling et al. (2007). Briefly, a 0.045 lpm flow of particle-laden air is sheathed in 0.45 lpm particle-free air. This flow is passed through a temperature-controlled vertical column with water-coated walls. Supersaturated conditions are produced in the column due to a temperature gradient produced by three differentially heated zones and the fact that water molecules diffuse more quickly than heat. The flow regime in the column is assumed to be laminar with a residence time of ~10 s. Validation of instrument performance is given in subsequent paragraphs. Once activated, the number and size distribution of droplets (from 0.75 to 10 μm diameter) is measured using an integrated optical particle counter (OPC).

Droplets exiting the CCNC were separated from unactivated particles using a pumped CVI (PCVI) previously described in the literature (Boulter et al., 2006; Kulkarni et al., 2011). A PCVI functions by drawing particles into the instrument with a vacuum pump. A flow of particle-free gas termed the counterflow is directed in a motion opposite the particle flow. In this way the counterflow creates an inertial barrier which stops particles below a specific cut-size so that they are removed by the flow to the pump. The rate of counterflow sets the inertial barrier and thus the cut-size. The counterflow

AMTD
4, 691–713, 2011

is a portion of the total flow added to the PCVI; the remainder forms an output or "sample flow" into which the particles above the cut-size become entrained (i.e., particles above the cut-size exit the PCVI within a different gas-phase environment than they entered; Boulter et al., 2006). In the case of these studies, the add flow was particle-free dry research-grade nitrogen (99.99% purity). The cut-size was set to allow passage of droplets but not unactivated particles. The dry nitrogen carrier gas thus caused evaporation of the condensed-phase water on the droplets so that only residual aerosol particles which initially formed the droplets in the CCNC remained in the sample flow. Described more fully in the following paragraphs, the PCVI used in these studies effectively separates ~2.5 μm and larger diameter droplets for input flow rates of ~5–10 lpm (Boulter et al., 2006; Kulkarni et al., 2011). A particle-free humidified "supplemental flow" was added to the ~0.5 lpm CCNC flow in order to produce the required PCVI input flow. This was done by directing the CCNC flow through a 4 mm id tube in the centerline of a 15 mm tube containing the supplemental flow. The supplemental flow was humidified by passing it through nafion tubing (Perma Pure, Toms River, NJ, PD Series) immersed in ultrapure 18.2 MΩ cm water so that droplets were not evaporated prior to the PCVI. The PCVI sample flow was 1.0 lpm for all experiments conducted here. The number density of particles in this was counted by directing 0.3 lpm to a condensation particle counter (CPC; TSI Inc., Shoreview, MN, model 3775). For experiments where particle size and composition were also measured, a HR-ToF AMS (Aerodyne Research Inc., Billerica, MA) or PALMS was attached in parallel. Both instruments utilize an aerodynamic inlet to focus particles into a narrow beam (Liu et al., 1995). Excess flow was removed with a vacuum pump.

The AMS has been described in the literature previously (Jayne, 2000; Jimenez et al., 2003; DeCarlo et al., 2006). Briefly, particles entrained in 0.1 lpm of flow are impacted onto a resistively heated (600–850 °C) ceramic oven. The AMS lens transmits particles with vacuum aerodynamic diameters of 70–500 nm with nearly 100% efficiency and diameters of 500–2000 nm with lower, but non negligible efficiency (Jayne, 2000). Bouncing of solid particles from the heater before volatilization may reduce the

AMTD
4, 691–713, 2011

AMS sampling efficiency further. Non-refractory components (operationally defined as components that vaporize in ~2 s) are volatilized on impact and the resultant vapor plume is ionized by electron impact at 70 eV. Ions are then orthogonally extracted at 20 kHz into a time of flight mass analyzer and detected after separation on a microchannel plate. For this study, the higher sensitivity "V" mode of the mass analyzer was employed. Mass spectra are analyzed with standard software as described in the literature to chemically resolve particle components (Allan et al., 2004). For the ambient studies, detection limits for the instrument as operated (1 min averaging) are approximately 0.1, 0.03, 0.02, 0.15 $\mu g\,m^{-3}$ for organics, nitrate, sulfate, and ammonium, respectively. A lower detection limit was achieved for PSLs (0.01 $\mu g\,m^{-3}$ nitrate equivalent mass at *m/z* 104) by monitoring a single intense peak that has little interference from other species and a low background.

PALMS has also been described in the literature previously (Cziczo et al., 2006). Particles in 0.3 lpm of flow are detected as they scatter light from two visible 532 nm YAG lasers set a known distance apart and this allows for a calculation of aerodynamic diameter. A 193 nm excimer laser is subsequently triggered to ablate and ionize the components. Positive or negative ions are sent through a reflectron mass spectrometer flight tube and detected as a function of mass. Particle size and chemical composition are thus recorded on the single particle level in situ and in real time. Optical detection and aerodynamic focusing restrict the particle size range to ~150–3000 nm, respectively. Within this range refractory (e.g., black carbon and mineral dust) and semi-volatile (e.g., sulfates and organics) can be resolved. Single particle mass spectrometers such as PALMS are not inherently quantitative but trends in ion signal can be used as an indication of relative abundance and particle fractions on the order of 1% are detectable (Cziczo, 2010 and references therein).

Initial tests were conducted to validate performance of the CCNC. Ammonium sulfate (Sigma-Aldrich, Saint Louis, MO, ReagentPlus Grade, >99% purity) was dissolved in 18.2 MΩ cm ultrapure water. Aerosol particles were produced by atomizing a 0.1 weight percent (wt%) solution (Atomizer; TSI Inc., Shoreview, MN, Model 3076).

AMTD
4, 691–713, 2011

In all cases, dry research-grade nitrogen was used as the carrier gas. Monodisperse sizes (i.e., mobility diameters) were produced using a differential mobility analyzer (DMA; TSI Inc., Shoreview, MN, Model 3080). Figure 2 shows the fraction of particles active as CCN as a function of supersaturation. Modeled CCN activation curves derived from the κ-Köhler model for ammonium sulfate are also plotted (Petters and Kreidenweis, 2007). The activated fraction appearing as a plateau at lower supersaturations corresponded to doubly charged particles (Rose et al., 2008) (e.g., 117 nm mode of doubly charged component on an electric mobility equivalent to 80 nm particles of +1 charge selected by DMA in Fig. 2). The size distributions of singly and doubly charged particles were measured by a scanning mobility particle sizer (SMPS; TSI Inc., Shoreview, MN, Model 3969) to find an activation curve of each component by assuming κ of 0.61. The difference in critical supersaturation (where 50% of the particles are CCN active) between modeled and observed data was never as high as 12%, validating performance of the CCNC. It should be noted that any higher order of multiply charged particles other than +2 charges were neglected due to their small population in this study. The droplet size distribution produced as a function of supersaturation for ammonium sulfate particles was also determined using the CCNC OPC (Fig. 3). Polystyrene latex (PSL) spheres (Duke Scientific, Palo Alto, CA) were produced in the same manner after dispersion in 18.2 MΩ MilliQ water. Note that, as shown in Fig. 2, PSLs exhibit significantly less activation than ammonium sulfate at a given size throughout the range of supersaturations considered here.

Two validation experiments were then conducted. First, monodisperse ammonium sulfate particles were produced and exposed to a variety of supersaturations in the CCNC and directed to the PCVI. A PCVI cut-size of ~2.5 micrometers was set by using a supplemental flow of 9.5 lpm and a counterflow of 3.0 lpm. As shown in Fig. 3, droplets of greater than 3 micrometers are produced for supersaturations of >0.5%. Figure 4 shows the output particle number density in the PCVI output flow; no particles were transmitted for a supersaturation of 0.25% whereas at 0.5% droplets were detected. The number density of these particles can be used to estimate a transmission

AMTD
4, 691–713, 2011

factor for this experiment:

$$T = \mathrm{CCN}\ (\mathrm{cm}^{-3}) \times \frac{0.045\ (\mathrm{lpm})}{0.495\ (\mathrm{lpm})} \times \frac{0.495\ (\mathrm{lpm})}{9.945\ (\mathrm{lpm})} \times 0.75 \times \frac{10\ (\mathrm{lpm})}{1\ (\mathrm{lpm})}$$
$$= \mathrm{CCN}\ (\mathrm{cm}^{-3}) \times 0.034 \quad (1)$$

The transmission T, in CCN residuals per cm^3 in the sample flow, is estimated starting with the concentration in the CCNC sample flow (0.045 lpm). This flow is combined with the CCNC sheath flow (0.45 lpm) and this is combined with the supplemental flow (9.5 lpm). The PCVI enhances particles by the ratio of the sample to input flow ratios (~10:1) although in practice only ~75% transmission is realized for these flow conditions due to impaction losses (Kulkarni et al., 2011). In total this results in a reduction of residual particle to initial droplet concentration by a factor of ~1:29 (i.e., 0.034). During the period of time given in Fig. 4b the average CCN concentration was 9365 cm^3. This corresponds to an estimate of ~319 which compares favorably to the CPC average value of 331 cm^3.

Two features of the transmission curve are noteworthy: (1) When droplets were produced at 0.75% supersaturation a lower number density was observed in the output flow. This is due to increased impaction losses for larger particles as described in Kulkarni et al. (2011). (2) Periodic spikes are apparent in the CPC data. Visual inspection showed that these spikes were due to occasional "sputtering" of water that is collected when droplets impact within the PCVI. These sputtering remnants likely contain a small amount of residual material from the impacting droplets although they were not detected by the AMS which has a lower threshold of ~60 nm.

In the second validation experiment two particulate flows, one of ammonium sulfate and the other of PSLs, were produced by two identical atomizers. Two identical DMAs were used to produce monodisperse flows of the same rate that were combined. Three periods were investigated (Fig. 5). During "Period I" the particle number density and ammonium sulfate and PSL signal exiting the DMAs (i.e., before the PCVI)

AMTD
4, 691–713, 2011

was determined (Panel Ia). The average mass spectrum during this period is given in Panel Ib. During Period II the combined particle flow was passed through the CCNC and PCVI when the saturation, 0.25%, was not sufficient to activate droplets from either particle type (see Fig. 2). Panels IIa and IIb are analogous to Ia and Ib but note that no particles are transmitted and only noise is observed in the mass spectrum. During Period III the saturation, 0.75%, was sufficient to activate droplets from ammonium sulfate large enough to pass the PCVI and particles are detected in the sample flow (Panel IIIa). Conversely, PSL spheres were not expected to activate (see Figs. 2 and 3); only ammonium sulfate and not PSL signal is evident in Panel IIIa and the mass spectrum in IIIb.

3 Atmospheric measurements

Coupled with two different mass spectroscopy techniques described above atmospheric measurements were conducted in Richland, WA to gain insight into the effect of composition on CCN formation. For experiments with the AMS, poly-dispersed ambient particles were exposed to supersaturated condition in the CCNC and droplet residual particles were passed to the AMS downstream of the PCVI. Ambient AMS measurements were also conducted immediately before and after the experiment with the CCNC and PCVI. As illustrated in Fig. 6, the time series of organic and inorganic mass were observed from ~09:30 to 12:00 Pacific Daylight Time (PDT) on 20 October 2010. The ambient temperature was ~13 °C with partly cloudy skies and moderate particle loadings (ambient particle concentration ~10 000 particles cm^{-3}) throughout the experiment. A series of supersaturations (0.25%, 0.4%, and 0.75%) in the CCNC were employed. A supersaturation of 0.4% produced 2255 droplets cm^{-3} and 76 residual particles cm^{-3} in the flow passed to the AMS.

When observing ambient particles, particle composition derived from the V mode of AMS measurements was dominated by organics and ammonium nitrate with a small ammonium sulfate contribution (Fig. 6 Panel I and III). When sampling behind the PCVI (Fig. 6 Panel II), dilution of aerosol particles in the PCVI will reduce the ammonium

AMTD
4, 691–713, 2011

and sulfate signals to below the AMS detection limit regardless of their activation in the CCNC. We see positive evidence that particles containing nitrate activated in the CCNC. Based on the PCVI dilution ratio, the organic signal of activated particles is expected to be near the AMS detection limit, assuming all organic containing particles activated. AMS observations show the organic signal hovering around the detection limit (Fig. 6 Panel IIb). Therefore, the role of organics in CCN activation is unclear on this particular day.

Experiments with the PALMS instrument were conducted in the same manner as for the AMS. An exemplary negative polarity mass spectrum of a residual particle of a droplet formed in the CCNC and separated from unactivated particles in the PCVI is shown in Fig. 7a. Peaks attributed to different species (e.g., sulfate, nitrate and organic) are specified. Data were collected as follows: 1000 positive and negative mass spectra of ambient particles were collected over ~10 min starting at 16:00 Pacific Standard Time on 9 November 2010. The ambient temperature was 5 °C with overcast skies and occasional drizzle and these conditions continued throughout the experiment. Ambient sampling was immediately followed by analysis of drop residue by connecting PALMS after the CCNC and PCVI for a period of 30 min. This resulted in the acquisition of 225 positive and 350 negative mass spectra. This period was immediately followed by collection of an additional 1000 positive and negative mass spectra. The CCNC was set at 0.5% saturation with respect to water producing an average of 500 droplets cm^{-3}; this resulted in 29 residual particles cm^{-3} in the flow passed to the PALMS instrument.

Average particle aerodynamic diameter and normalized signal attributed to sulfate, nitrate and organic are presented in Fig. 7b. Period I is the initial ambient data sample, period II is while PALMS was connected to the CCNC and PCVI, and period III is the final ambient sample. The peak analysis corresponds to the subset of negative polarity mass spectra acquired whereas the size information uses all mass spectra. The droplet residual material is somewhat larger than the ambient aerosol size although these correspond to the subset of CCN residuals within the PALMS size range. The total of all mass spectral peaks is 1 with the fraction attributed to sulfate, nitrate and

AMTD
4, 691–713, 2011

organic presented in Fig. 7b for each time period; note that these species make up the majority, from 73–80%, of the total ion current produced in each period. Sulfate is slightly enhanced in the residual particles whereas nitrate is slightly reduced. Organic components do not display a clear trend.

4 Conclusions

We have connected a CCN chamber to a PCVI in order to separate droplets from unactivated interstitial aerosol. The flow added to the PCVI was at low relative humidity so that droplets were evaporated and only residual particles were entrained in the sample flow. The number of residual particles compared favorably with the droplets produced in the CCN chamber, with particle losses on the order of 25%, consistent with what has been observed previously using PCVIs. Two validation experiments were performed. First, various supersaturations were used to produce droplets of different sizes. Only when droplets larger than the cut-size of the PCVI were formed were residual particles observed in the sample flow. This verified that only droplets with sufficient size passed through the counterflow virtual impactor for subsequent analysis. Second, an external mixture of ammonium sulfate and PSL monodisperse particles was also exposed to a supersaturation which would activate only ammonium sulfate but not the PSLs. The mass spectrum observed with an AMS after separation indicated only ammonium sulfate, validating separation of droplets from unactivated particles. To our knowledge this is the first time a commercial DMT CCN chamber has been coupled to a PCVI and mass spectrometer and we are aware of only one other such instrumental combination using a custom CCN chamber (Slowik et al., 2011).

Two mass spectrometers were then used for ambient sampling. An AMS, which provides a quantitative measurement of non-refractory aerosol components of 70–1000 nm diameter particles, showed little chemical differentiation between ambient particles and the subset that were activated in the CCNC. However, particle loadings were relatively low and dilution from the PCVI alone is expected to reduce the ammonium

AMTD
4, 691–713, 2011

and sulfate signal to below the AMS detection limit. For this particular day, particles containing ammonium nitrate were clearly observed to activate in the CCNC. The role of organics in activation remains unclear. One key limitation of this technique was that sufficient particle mass loading had to be present in the sample flow for the AMS to acquire meaningful data. Because separation of droplets by the PCVI requires that the ambient aerosol be diluted by a factor of ∼30, ambient particle mass loadings of 1–5 μg m^{-3} (depending on particle composition) are required to chemically differentiate particle CCN activity by the AMS. The AMS coupled with the PCVI can provide a quantitative measurement of bulk aerosol composition with high time resolution, however, these results suggest that PCVI-AMS combination may not be the optimal technique to observe the influence of composition on cloud droplet formation in the absence of relatively high particle mass loadings. The PALMS instrument, which provides universal component detection on a single particle basis but only on a qualitative level from ∼150–3000 nm diameter, showed a slight increase in the size of particles which were activated as droplets. Slight chemical differences were observed with a small enhancement of sulfate and decrease in nitrate observed in the droplet residuals.

These two mass spectrometers proved to be complementary instruments. The AMS was able to probe particle sizes near the activation threshold and produced quantitative data. PALMS was able to universally detect aerosol components, including mineral dust and black carbon, and acquired single particle data even when only a few droplet residuals per cm^3 were present in the sample flow. We believe that for most ambient sampling use of both techniques will be required to fully characterize the effect of aerosol composition on cloud droplet formation.

Acknowledgements. Funding for this work was provided by the Pacific Northwest National Laboratory Aerosol Climate Initiative and Goethe-University Frankfurt am Main. The authors wish to thank Gourihar Kulkarni for useful discussions.

AMTD
4, 691–713, 2011

References

Albrecht, B. A.: Aerosols, cloud microphysics and fractional cloudiness, Science, 245, 1227–1230, 1989.

Allan, J. D., Delia, A. E., Coe, H., Bower, K. N., Alfarra, M. R., Jimenez, J. L., Middlebrook, A. M., Drewnick, F., Onasch, T. B., Canagaratna, M. R., Jayne, J. T., and Worsnop, D. R.: A generalised method for the extraction of chemically resolved mass spectra from aerodyne aerosol mass spectrometer data, J. Aeros. Sci., 35, 909–922, 2004.

Boulter, J. E., Cziczo, D. J., Middlebrook, A. M., Thomson, D. S., and Murphy, D. M.: Design and performance of a pumped counterflow virtual impactor, Aerosol Sci. Tech., 40, 969–976, 2006.

Cziczo, D. J.: Atmospheric aerosol analysis by laser ionization, in: The Encyclopedia of Mass Spectrometry, Vol. 5, edited by: Gross, M. L., Carioli, R. M., Beauchemin, D., and Matthews, D. E., Elsevir, Amsterdam, The Netherlands, 2010.

Cziczo, D. J., Thomson, D. S., Thompson, T., DeMott, P. J., and Murphy, D. M.: Aerosol mass spectrometry studies of ice nuclei and other low number density particles, Int. J. Mass Spectrom., 258, 21–31, 2006.

DeCarlo, P. F., Dunlea, E. J., Kimmel, J. R., Aiken, A. C., Sueper, D., Crounse, J., Wennberg, P. O., Emmons, L., Shinozuka, Y., Clarke, A., Zhou, J., Tomlinson, J., Collins, D. R., Knapp, D., Weinheimer, A. J., Montzka, D. D., Campos, T., and Jimenez, J. L.: Fast airborne aerosol size and chemistry measurements above Mexico City and Central Mexico during the MILAGRO campaign, Atmos. Chem. Phys., 8, 4027–4048, doi:10.5194/acp-8-4027-2008, 2008.

Dusek, U., Frank, G., Hildebrandt, L., Curtius, J., Schneider, J., Walter, S., Chand, D., Drewnick, F., Hings, S., Jung, D., Borrmann, S., and Andreae, M. O.: Size matters more than chemistry for cloud-nucleating ability of aerosol particles, Science, 312, 1375–1378, 2006.

Gard, E. E., Kleeman, M. J., Gross, D. S., Hughes, L. S., Allen, J. O., Morrical, B. D., Fergenson, D. P., Dienes, T., Galli, M. E., Johnson, R. J., Cass, G. R., and Prather, K. A.: Direct observation of heterogeneous chemistry in the atmosphere, Science, 279, 1184–1187, 1998.

Jimenez, J. L., Jayne, J. T., Shi, Q., Kolb, C. E., Worsnop, D. R., Yourshaw, I., Seinfeld, J. H., Flagan, R. C., Zhang, X., Smith, K. A., Morris, J., and Davidovits, P.: Ambient aerosol sampling with an aerosol mass spectrometer, J. Geophys. Res., 108(D7), 8425, doi:10.1029/2001JD001213, 2003.

Kulkarni, G., Pekour, M., Afchine, A., Murphy, D. M., and Cziczo, D. J.: Comparison of exper-

AMTD
4, 691–713, 2011

imental and numerical studies of the performance characteristics of a pumped counterflow virtual impactor, Aerosol Sci. Tech., 45, 382–392, 2011.
Lance, S., Medina, J., Smith, J. N., and Nenes, A.: Mapping the operation of the DMT continuous flow CCN counter, Aerosol Sci. Tech., 40, 242–254, 2006.
Laskin, A., Wietsma, T. W., Krueger, B. J., and Grassian,V. H.: Heterogeneous chemistry of individual mineral dust particles with nitric acid: A combined CCSEM/EDX, ESEM, and ICP-MS study, J. Geophys. Res., 110, D10208, doi:10.1029/2004JD005206, 2005.
Liu, P., Ziemann, P. J., Kittelson, D. B., and McMurry, P. H.: Generating particle beams of controlled dimensions and divergence, 1. Theory of particle motion in aerodynamic lenses and nozzle expansions, Aerosol Sci. Tech., 22, 293–313, 1995.
Lohmann, U. and Feichter, J.: Global indirect aerosol effects: a review, Atmos. Chem. Phys., 5, 715–737, doi:10.5194/acp-5-715-2005, 2005.
IPCC.: Climate Change 2007: The Physical Science Basis. Contribution of Working Group I to the Fourth Assessment Report of the Intergovernmental Panel on Climate Change, Cambridge University Press, Cambridge, UK and New York, NY, USA, 2007.
Moore, R. H., Nenes, A., and Medina, J.: Scanning mobility CCN analysis – A method for fast measurements of size-resolved CCN distributions and activation kinetics, Aerosol Sci. Tech., 44, 861–871, 2010.
Murphy, D. M., Thomson, D. S., and Mahoney, M. J.: In situ measurements of organics, meteoritic material, mercury, and other elements in aerosols at 5 to 19 kilometers, Science, 282, 1664–1669, 1998.
Nenes, A., Charlson, R. J., Facchini, M. C., Kulmala, M. Laaksonen, A., and Seinfeld, J. H.: Can chemical effects on cloud droplet number rival the first indirect effect?, Geophys. Res. Lett., 29(17), 1848, doi:10.1029/2002GL015295, 2002.
Petters, M. D. and Kreidenweis, S. M.: A single parameter representation of hygroscopic growth and cloud condensation nucleus activity, Atmos. Chem. Phys., 7, 1961–1971, doi:10.5194/acp-7-1961-2007, 2007.
Roberts, G. and Nenes, A.: Continuous-flow streamwise thermal-gradient CCN chamber for atmospheric measurements, Aerosol Sci. Tech., 39(3), 206–221, 2005.
Rose, D., Gunthe, S. S., Mikhailov, E., Frank, G. P., Dusek, U., Andreae, M. O., and Pöschl, U.: Calibration and measurement uncertainties of a continuous-flow cloud condensation nuclei counter (DMT-CCNC): CCN activation of ammonium sulfate and sodium chloride aerosol particles in theory and experiment, Atmos. Chem. Phys., 8, 1153–1179, doi:10.5194/acp-8-

AMTD
4, 691–713, 2011

1153-2008, 2008.
Rose, D., Nowak, A., Achtert, P., Wiedensohler, A., Hu, M., Shao, M., Zhang, Y., Andreae, M. O., and Pöschl, U.: Cloud condensation nuclei in polluted air and biomass burning smoke near the mega-city Guangzhou, China Part 1: Size-resolved measurements and implications for the modeling of aerosol particle hygroscopicity and CCN activity, Atmos. Chem. Phys., 10, 3365–3383, doi:10.5194/acp-10-3365-2010, 2010.
Seinfeld, J. H. and Pandis, S. N.: Atmospheric Chemistry and Physics, John Wiley & Sons, New York, 2006.
Shilling, J. E., King, S. M., Mochida, M., and Martin, S. T.: Mass spectral evidence that small changes in composition caused by oxidative aging processes alter aerosol CCN properties. J. Phys. Chem. A, 111(17), 3358–3368, 2007.
Slowik, J. G., Cziczo, D. J., and Abbatt, J. P. D.: Analysis of cloud condensation nuclei composition and growth kinetics using a pumped counterflow virtual impactor and aerosol mass spectrometer, Atmos. Meas. Tech., Discuss., 4, 285–313, 2011.
Squires, P.: The microstructure and colloidal stability of warm clouds. I. The relation between structure and stability, Tellus, 10, 256–271, 1958.
Stevens, B. and Feingold, G.: Untangling aerosol effects on clouds and precipitation in a buffered system, Nature, 461, 607–613, 2009.
Twomey, S.: Pollution and the planetary albedo, Atmos. Environ., 8(12), 1251–1256, 1974.

AMTD
4, 691–713, 2011

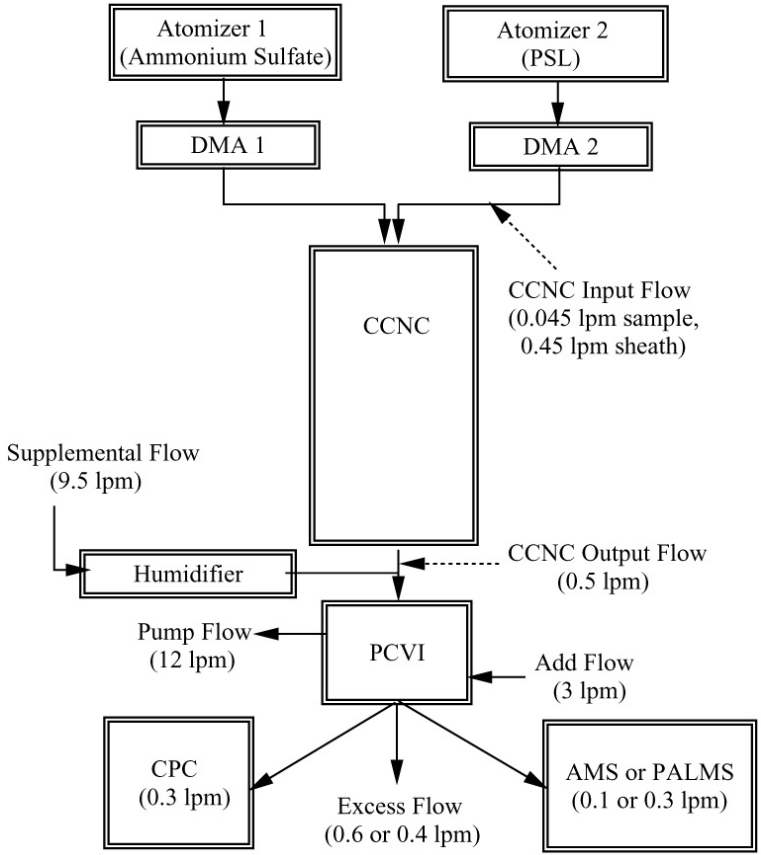

Fig. 1. Schematic of the experimental setup.

AMTD
4, 691–713, 2011

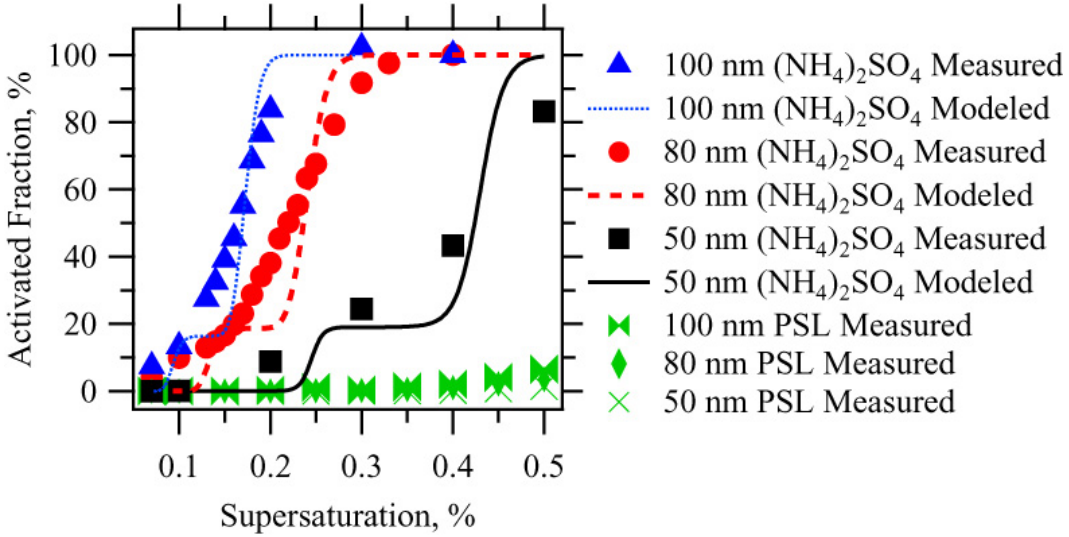

Fig. 2. Fraction of aerosols active as CCN as a function of supersaturation. The size and composition of the aerosol is differentiated by the shapes given in the legend.

AMTD
4, 691–713, 2011

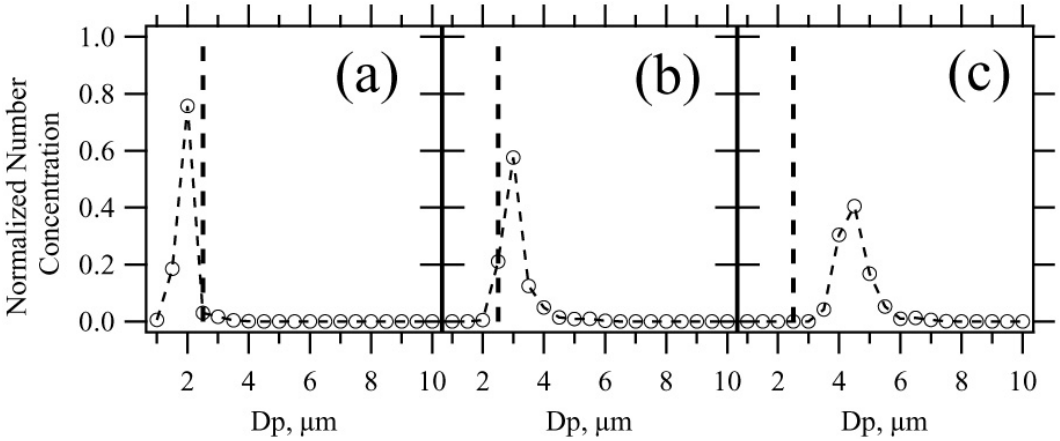

Fig. 3. Droplet size distribution as a function of supersaturation, **(a)** 0.25%, **(b)** 0.5%, and **(c)** 0.75%, for ammonium sulfate. Note that vertical extension of dashed line in each panel represents the D_{50} cut-size of ~2.5 micrometer diameter for the PCVI.

AMTD
4, 691–713, 2011

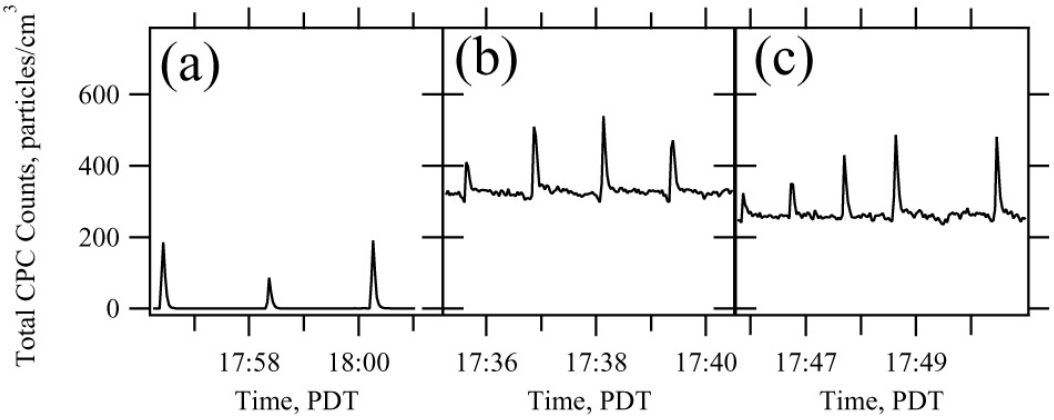

Fig. 4. Transmitted particle number density after the PCVI as a function of time for various supersaturations. During "Period **(a)**" the droplets remained below the cut-size and no particles were transmitted (supersaturation 0.25%). During Period **(b)** the ammonium sulfate particles activated into droplets larger than the cut-size (0.5%). During Period **(c)** droplets grew to a size where impaction losses increased over those in Period (b) (0.75%; Kulkarni et al., 2011). See Fig. 3 for relevant droplet sizes.

AMTD
4, 691–713, 2011

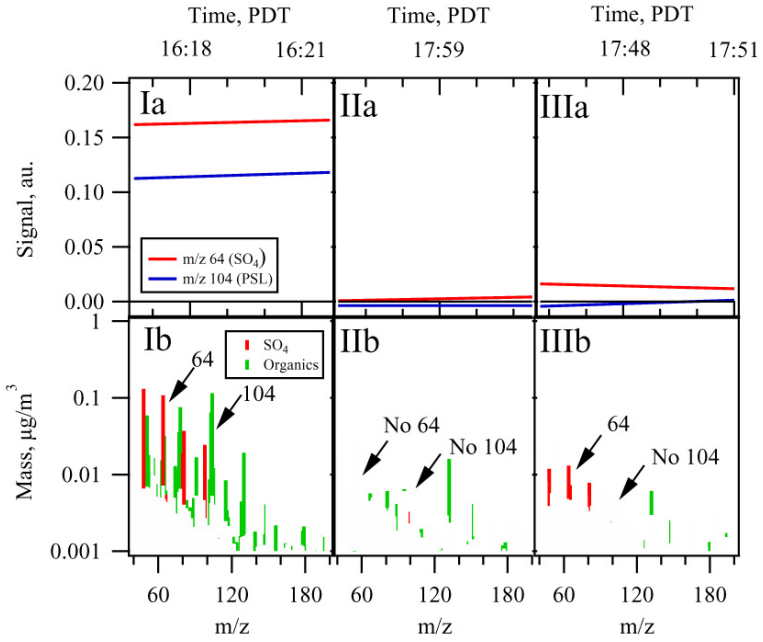

Fig. 5. Aerosol concentration and composition for experiments where ammonium sulfate and PSL spheres were externally mixed. Panel **(Ia)** is the time series of sulfate and PSL mass spectra signal before the CCNC and PCVI. The AMS average mass spectrum during this period is given in panel **(Ib)**. Panel **(IIa)** is the same quantities as in Ia but after the CCNC and PCVI at 0.25% saturation when the saturation was not sufficient to activate droplets from either particle type (see Fig. 2). The concurrent spectrum is given in Panel **(IIb)**. Panel **(III)** shows that the saturation (0.75%) was sufficient to activate droplets from ammonium sulfate and the formed droplets were large enough to pass the PCVI whereas PSL spheres did not activate (see Figs. 2 and 3). Note that only ammonium sulfate, and not PSL signal, is evident in Panel **(IIIa)** and the mass spectrum in **(IIIb)**.

AMTD
4, 691–713, 2011

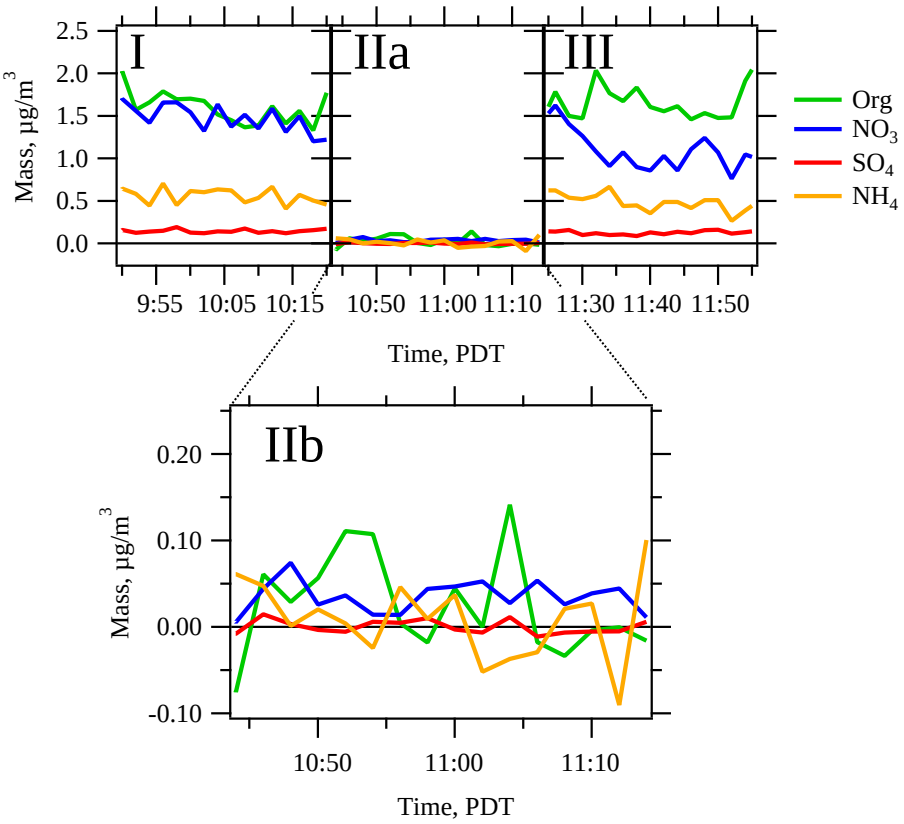

Fig. 6. Time series of organic and inorganic mass determined by AMS measurements. Period **(I)** is ambient data. Period **(II)** is the mass measurement after the CCNC and PCVI immediately after Period I. Period **(III)** is ambient data immediately after Period II. Note that Fig. 6 **(IIa)** has a consistent mass scale with I and III, and Fig. 6 **(IIb)** has a 10× mass scale.

AMTD
4, 691–713, 2011

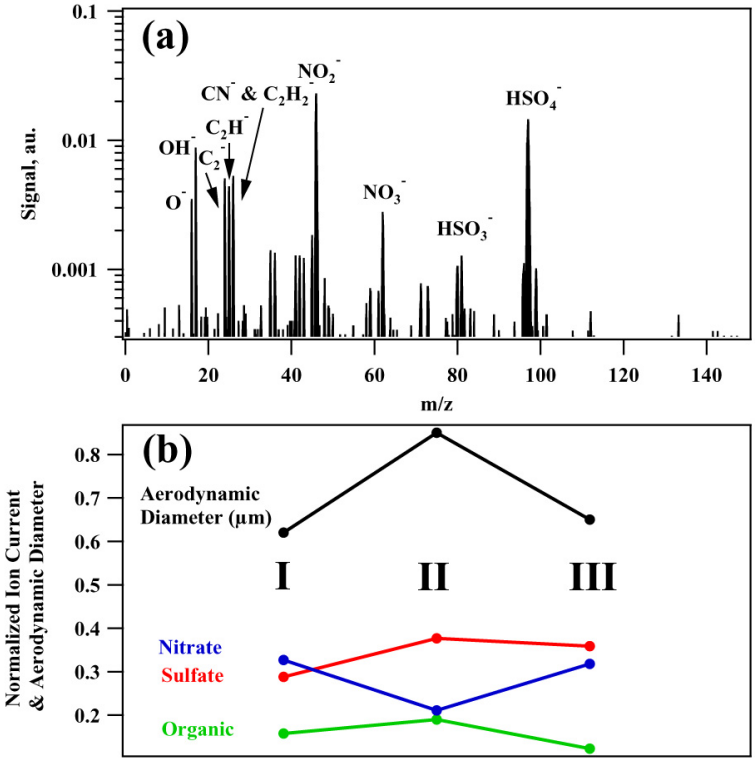

Fig. 7. Negative polarity mass spectrum of a CCN residual using the PALMS instrument (panel **a**). Sulfate, nitrate and organic peaks are identified. Time series averages of aerodynamic diameter and sulfate, nitrate and organic signal (panel **b**). Period I is ambient data. Period II is from mass spectra after the CCNC and PCVI immediately after Period I. Period III is ambient data immediately after Period II. See text for details.

AMTD
4, 691–713, 2011